Novel Mechanism for Triplet State Formation in Short Distance Covalently Linked Radical Ion Pairs

Gary P. Wiederrecht,[†] Walter A. Svec,[†] Michael R. Wasielewski,*[,‡] Tamar Galili,[§] and Haim Levanon*[,§]

Contribution from the Chemistry Division, Argonne National Laboratory, Argonne, Illinois, 60439-4831, Department of Chemistry, Northwestern University, Evanston, Illinois 60208-3113, and Department of Physical Chemistry and The Farkas Center for Light-Induced Processes, The Hebrew University of Jerusalem, Jerusalem 91904, Israel

Received February 23, 2000. Revised Manuscript Received June 28, 2000

Abstract: We report on a series of electron donor−acceptor (D-A) dyads that undergo singlet-initiated charge separation to produce a strongly spin coupled radical ion pair that subsequently undergoes charge recombination to produce a triplet state with unusual spin polarization. The molecules consist of either a 4-(*N*-piperidinyl)-naphthalene-1,8-imide (6P) or 4-(*N*-pyrrolidinyl)naphthalene-1,8-imide (5P) donor and a 1,8:4,5-naphthalene-diimide (NI) or pyromellitimide (PI) acceptor. Selective photoexcitation of D within D-−A produces the radical ion pair $^1[D^{\bullet+}\text{-}A^{\bullet-}]$ quantitatively. This is followed by the formation of $^3[D^{\bullet+}\text{-}A^{\bullet-}]$ via singlet−triplet mixing within the radical pair. Radical pair intersystem crossing (RP-ISC) leads to charge recombination to yield [D-^{3*}A] or [^{3*}D-A]. Time-resolved optical absorption and emission spectroscopy is coupled with EPR spectroscopy to characterize the mechanism of the nearly quantitative initial charge separation reaction and the subsequent radical ion pair recombination reaction leading to the unusually spin polarized triplet state. These radical pairs also possess charge transfer emission bands that aid in the data analysis. The small number of previously reported covalent donor−acceptor systems that yield a triplet state from radical ion pair recombination use multistep charge separation reactions to achieve a ≥20 Å spacing between the oxidized donor and reduced acceptor. These examples have small exchange couplings, *J*, within the radical pair, so that S-T_0 mixing between the radical pair energy levels occurs. In the strongly coupled systems described here, we show that the triplet states are formed by means of both S-T_0 and S-T_{-1} mixing, producing novel spin-polarized EPR spectra characterized by anisotropic spin lattice relaxation.

Introduction

The spin dynamics of the primary photochemistry of photosynthetic reaction centers has proven difficult to simulate in artificial photosynthetic model systems.[1] A particularly interesting aspect of primary photosynthesis is the back electron-transfer reaction that produces a triplet state of the initial bacteriochlorophyll or chlorophyll donors within isolated prereduced bacterial or green plant photosystem II reaction centers. This triplet state has a unique spin polarization that has been detected through electron paramagnetic resonance (EPR).[2−5] However, despite many attempts, this process has only been reproduced in two artificial covalently bound donor−spacer−acceptor systems.[6−8] In these systems photoexcitation is followed by sequential charge transfer to create the singlet-initiated radical pair $^1[D^{\bullet+}\text{-}A_1\text{-}A_2^{\bullet-}]$. In both known systems, the donor−acceptor distances are greater than 20 Å, leading to the formation of a spin-correlated radical pair, i.e., $^{1,3}[D^{\bullet+}\text{-}A_1\text{-}A_2^{\bullet-}]$. Radical ion pair recombination within $^3[D^{\bullet+}\text{-}A_1\text{-}A_2^{\bullet-}]$ yields $^{3*}[D\text{-}A_1\text{-}A_2]$, where the triplet state can be localized on the D or A_2 moieties. In all of these reactions the radical pair spectra show non-Boltzmann populations of the spin states, exhibiting spin-polarized EPR spectra characteristic of the mechanism of their formation.

In contrast to the long distance electron transfer systems described above, we recently reported a donor−acceptor molecule (6P-NI in Figure 1) with a short electron-transfer distance of 11 Å that also forms a ^{3*}[D-A] state following back electron transfer.[9] In this molecule, a single step electron-transfer reaction occurs following photoexcitation of the donor, 6P, to produce a ^{3*}[D-A] state via the following mechanism: ^{1*}6P-NI → $^1(6P^{+}\text{-}NI^{-})$ → $^3(6P^{+}\text{-}NI^{-})$ → ^{3*}(6P-NI). However, due to the high value of the exchange integral, *J*, within the radical ion pair, this molecule has a unique back electron-transfer mechanism as evidenced by the different electron spin polarization (ESP) pattern of ^{3*}[D-A] relative to those for the molecules with longer radical ion pair distances reported previously.[6−8]

[†] Argonne National Laboratory.
[‡] Northwestern University.
[§] The Hebrew University of Jerusalem.

(1) Levanon, H.; Galili, T.; Regev, A.; Wiederrecht, G. P.; Svec, W. A.; Wasielewski, M. R. *J. Am. Chem. Soc.* **1998**, *120*, 6366−6373.
(2) Thurnauer, M. C.; Katz, J. J.; Norris, J. R. *Proc. Natl. Acad. Sci. U.S.A.* **1975**, *72*, 3270.
(3) Dutton, P. L.; Leigh, J. S.; Seibert, M. *Biochem. Biophys. Res. Commun.* **1972**, *46*, 406.
(4) Regev, A.; Nechushtai, R.; Levanon, H.; Thornber, J. P. *J. Phys. Chem* **1989**, *93*, 2421.
(5) Rutherford, A. W.; Paterson, D. R.; Mullet, J. E. *Biochim. Biophys. Acta* **1981**, *635*, 205.
(6) Hasharoni, K.; Levanon, H.; Greenfield, S. R.; Gosztola, D. J.; Svec, W. A.; Wasielewski, M. R. *J. Am. Chem. Soc.* **1995**, *117*, 8055−8056.
(7) Hasharoni, K.; Levanon, H.; Greenfield, S. R.; Gosztola, D. J.; Svec, W. A.; Wasielewski, M. R. *J. Am. Chem. Soc.* **1996**, *118*, 10228−35.
(8) Carbonera, D.; DiValentin, M.; Corvaja, C.; Agostini, G.; Giacometti, G.; Liddell, P. A.; Kuciauskas, D.; Moore, A. L.; Moore, T. A.; Gust, D. *J. Am. Chem. Soc.* **1998**, *120*, 4398−4405.
(9) Wiederrecht, G. P.; Svec, W. A.; Wasielewski, M. R.; Galili, T.; Levanon, H. *J. Am. Chem. Soc.* **1999**, *121*, 7726−7.

10.1021/ja000662o CCC: $19.00
Published on Web 09/26/2000

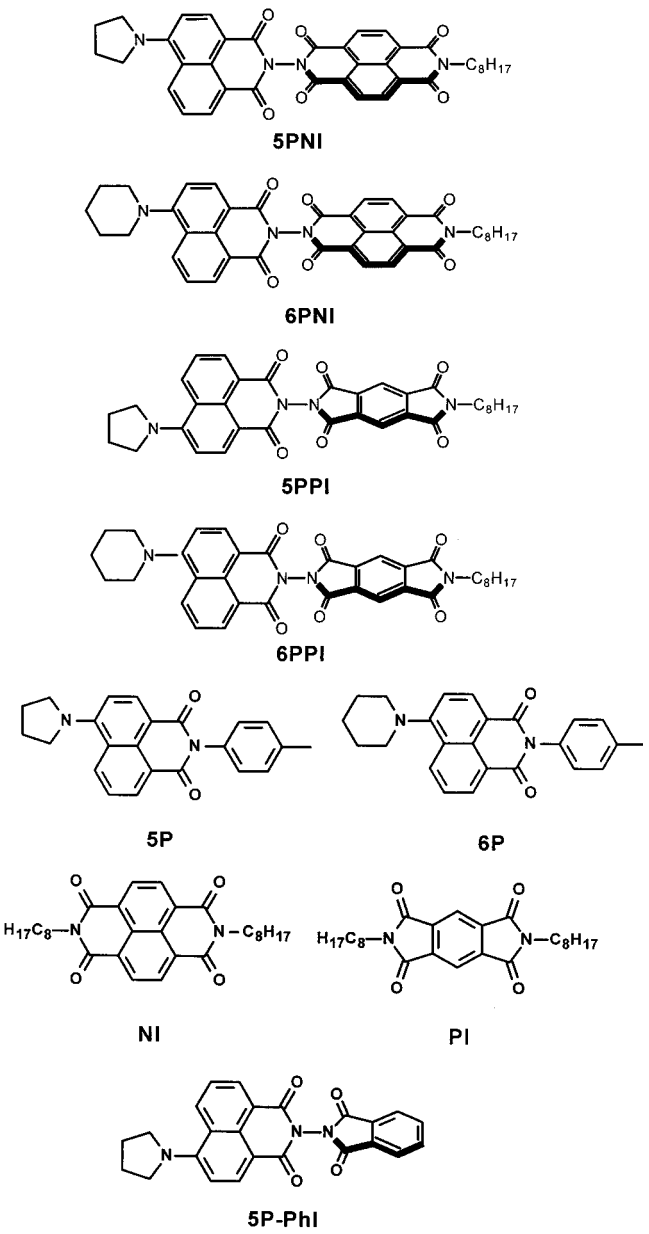

Figure 1. The (a) donor−acceptor dyads and (b) control molecules are illustrated.

A polarization pattern similar to that observed for 6P-NI was found following photoexcitation of 10-(1- and 2-naphthyl)-9-methylacridinium ions in solid solutions at temperatures from about 100−300 K.[10] The proposed mechanism for the unusual ESP pattern observed for these molecules is direct formation of the locally excited acridinium triplet state from the singlet radical pair. In these molecules an intermediate triplet radical pair state is not observed by TREPR. This mechanism is similar to one that has been proposed previously for aniline−anthracene[11] and porphyrin−quinone[12] donor−acceptor molecules. It relies on the fact that electron transfer from a donor π system, which is held in an orientation perpendicular to that of the acceptor, provides a significant change in orbital angular momentum requiring a rapid spin flip to conserve energy. This mechanism is analogous to ordinary spin−orbit induced intersystem crossing, except that the donor and acceptor π orbitals are on two separate molecules or two widely separated parts of the same molecule. The fact that the triplet radical pair is clearly observed by TREPR following photoexcitation of our molecules in liquid crystal solvents over a wide range of temperatures rules out the spin−orbit mechanism observed for acridinium triplet formation.

Table 1. The Oxidation and Reduction Potentials of the Donors and Acceptors in Butyronitrile[a]

molecule	E_{OX} (V vs SCE)	E_{RED} (V vs SCE)
6P	1.23	−1.41
5P	1.04	−1.55
NI	N/A	−0.50
PI	N/A	−0.79

[a] No change is observed for the covalently linked chromophores within the dyads

We now report an extended study of a series of short distance, covalently bound D-A molecules that undergo back electron transfer to a triplet state, and are thus designed to shed insight on the novel mechanism for charge recombination under these conditions. The new series of molecules also exhibits charge-transfer emission bands that permit overlapping optical and EPR experiments for analyzing the unique photophysics and photochemistry of these D-A systems. A critical aspect of this study is that liquid crystals (LCs) were utilized as solvents to slow the electron-transfer rates in these molecules, permitting the employment of time-resolved EPR (TREPR) spectroscopy to characterize their spin dynamics.[13]

Experimental Section

Figure 1 illustrates the molecules used for this study. A total of four dyads were synthesized, consisting of either 4-(*N*-piperidinyl)naphthalene-1,8-imide (6P) or 4-(*N*-pyrrolidinyl)naphthalene-1,8-imide (5P) as donors and 1,8:4,5-naphthalenediimide (NI) or pyromellitimide (PI) as acceptors. The syntheses of dyads 5P-PI, 6P-PI, and 6P-NI are described elsewhere.[9,14] Control experiments were also performed on the separate donor (5P, 6P) and acceptor (PI, NI) molecules. Additionally, a molecule with a pseudoacceptor, designated as 5P-PhI, was studied as a control molecule that cannot undergo electron transfer because of the high reduction potential of PhI. The syntheses of 5P-NI and 5P-PPhI are given in the Supporting Information.

The 5P and 6P donor molecules have absorption maxima at 432 and 400 nm, respectively. For the optical and TREPR studies, selective photoexcitation of the donor is accomplished through photoexcitation at 420 nm. The extinction coefficients for the donors ($e = 12\,000$ M^{-1} cm^{-1}) relative to NI are ∼20:1 at 420 nm, but any photoexcitation of NI is followed by energy transfer to the donor on a few picosecond time scale.[14] PI does not absorb at 420 nm. The dyad moieties were also chosen in part for their favorable redox characteristics, and Table 1 illustrates the redox characteristics of the donors and acceptors in butyronitrile. There is no measurable change in the redox characteristics of the donors and acceptors when they are covalently bound.

Continuous wave (CW) direct detection TREPR measurements were performed on the dyads and control molecules embedded and oriented in a LC (E-7, Merck Ltd.).[15] The compounds were first dissolved in toluene (∼1 mM), which was then evaporated, and the LC was introduced into 4 mm o.d. Pyrex tubes. The samples were degassed on a vacuum line by several freeze−pump−thaw cycles. TREPR measurements were carried out on a Bruker ESP-380 spectrometer with the field modulation disconnected and a time resolution of ∼200 ns.[16] Temperatures were maintained by using a variable-temperature nitrogen

(10) Willigan, H. v.; II, G. J.; Farahat, M. S. *J. Phys. Chem.* **1996**, *100*, 3312−16.
(11) Okada, T.; Karaki, I.; Matsuzawa, E.; Mataga, N.; Sakata, Y.; Misumi, S. *J. Phys. Chem.* **1981**, *85*, 3957.
(12) Wasielewski, M. R.; Johnson, D. G.; Svec, W. A.; Kersey, K. M.; Minsek, D. W. *J. Am. Chem. Soc.* **1988**, *110*, 7219−21.
(13) Hasharoni, K.; Levanon, H. *J. Phys. Chem.* **1995**, *99*, 4875−78.
(14) Debreczeny, M. P.; Svec, W. A.; Wasielewski, M. R. *New J. Chem.* **1996**, *20*, 815−828.
(15) Levanon, H. *Rev. Chem. Intermed.* **1987**, *8*, 287.
(16) Gonen, O.; Levanon, H. *J. Phys. Chem.* **1985**, *89*, 1637−43.

Table 2. The Magnetic, Relative Population Rates, and Distribution Parameters Are Given for [^{3}*D-A] or [D-^{3}*A]

molecule	$\|D\|^a$	$\|E\|^a$	A_x:A_y:A_z	σ_θ'	ϕ_0	σ_ϕ
5P	495	28	0.2:0.8:0.0	30	45	10
NI	743	12	0.2 : 0.8:0.0	34	45	5
5P-PI	645	70	0.2:0.0:0.8	35	65	10
6P-PI	645	84	0.2:0.0:0.8	45	65	10
5P-NI	757	4.7	0.8:0.2:0.0	45	70	15
6P-NI	748	4.7	0.8:0.2:0.0	45	60	15

[a] Units: $\times 10^{-4}$ cm^{-1}. Estimated errors $\pm$5%.

flow dewar in the EPR resonator. Samples were excited at 420 nm ($\sim$2 mJ/pulse at a repetition rate of 20 Hz) by a dye laser (Continuum, TDL-60, Stilbene 420) pumped by the third harmonic of a Nd:Yag laser (Continuum, 661-20).

The phase transition temperatures for E-7 are

$$\text{crystalline} \xrightarrow{210\ \text{K}} \text{soft glass} \xrightarrow{263\ \text{K}} \text{nematic} \xrightarrow{333\ \text{K}} \text{isotropic}$$

In the crystalline phase, two sample orientations with respect to the magnetic field were studied, **L**$\|$**B** and **L**$\perp$**B**, where **L** is the LC director and **B** is the external magnetic field. When the initial alignment of the sample is **L**$\|$**B**, spectra for **L**$\perp$**B** were obtained by rotation of the sample in the microwave cavity by $\pi/2$ about an axis perpendicular to the external magnetic field **B**. In the soft glass and fluid nematic phases, where molecular motion is permitted, rotation of the sample has no effect, since molecular reorientation brings the sample back to its initial parallel orientation. Thus, at these relatively elevated temperatures, only the **L**$\|$**B** orientation of the sample was studied.

Analysis of the EPR line shape and the dynamics of the photoexcited triplets oriented in different environments, i.e., isotropic and uniaxial LCs, are described elsewhere.[17,18] The extracted ZFS parameters, D and E, and the corresponding relative triplet population rates, A_x, A_y, and A_z, are given in Table 2. The preferred in-plane orientation of the guest molecules with respect to the director **L** in the LC is given by the angle ϕ_0 with the variance σ_ϕ. The variance $\sigma_{\theta'}$ is also given for the anisotropic out-of-plane angles.

Optical spectroscopy measurements were also performed to observe the photophysical properties that occur faster than the 200 ns time resolution of the TREPR spectrometer. The spectroscopies included ns and fs transient absorption, CW fluorescence and phosphorescence, and time correlated single photon counting (TCSPC). The ns and fs transient absorption spectrometers have been described elsewhere.[19,20] The TCSPC spectrometer was used to determine the emission time constants and spectral characteristics of the charge-transfer emission bands of 5P-NI and 6P-NI. The experimental setup consists of a Ti:sapphire laser that is acoustooptically cavity dumped at 800 kHz. Home-built RF electronics are used to control the phase of the acoustic wave relative to the optical pulse within the oscillator. This phase matching technique permits nearly 70% of the pulse energy to be cavity dumped, resulting in up to 50 nJ/pulse.[21,22] The output is frequency doubled to 400 nm and used to pump 3 mm thick samples within a liquid nitrogen dewar. A Hamamatsu R3809U multichannel plate photomultiplier in conjunction with an EG&G 9308 time analyzer and 9307 discriminators permit a time resolution of 50 ps. Three-dimensional spectral data was obtained by stepping the detection monochromator and obtaining a kinetic scan at each wavelength.

Results and Discussion

Optical Spectroscopy of the Dyads in Low-Temperature Organic Glasses. Optical studies were performed to characterize the charge separation and charge recombination times at low temperature in 2-MTHF glass, as measured by ns and fs transient absorption or emission spectroscopy. There are three factors that make these molecules particularly amenable to optical studies. The first is that the reduced PI and NI acceptors in the dyads have large and narrow absorption bands at 710 and 480 nm, respectively, permitting unambiguous observation of the formation and decay of the ion pairs through transient absorption spectroscopy. The second factor results from the observation of intense phosphorescence of a triplet state that we show is generated by back electron transfer. The third is that the radical pairs possess charge-transfer emission bands that permit the energy levels of the charge-separated states to be determined.

Table 3. Charge Recombination Times (τ_{CR}) Measured through Transient Absorption (TA) and Emission (Em) Spectroscopy, along with Their Averaged Values along with Phosphorescence Lifetimes (τ_{PH}) of the ^{3}*[D-A] Molecules at 77 K in 2-MTHF

	τ_{CR}, ns			
dyad	TA	Em	avg	τ_{PH},ms
5P-NI	61	55	58	63 (302, 30%)
6P-NI	51	39	45	61
5P-PI	81	65	73	560
6P-PI	64	N/A	64	330

Concerning factor one, fs and ns transient absorption spectroscopy has previously been used to follow the photoinduced reaction of [^{1}*6P$-$NI] $\rightarrow$ ^{1,3}[6P$^{\bullet+}$-NI$^{\bullet-}$] $\rightarrow$ [6P-^{3}*NI] in 77K 2-MTHF glass.[9] The experiments showed that the 480 nm absorption band of the reduced NI$^{\bullet-}$ species was present on a subpicosecond time scale, so that the charge separated state was formed with 100% quantum yield. For the present work, we ascertained the kinetics and spectral data for all of the dyads, which are shown in Table 3. All of the dyads show similar characteristics, i.e., subpicosecond formation times as determined by the appearance of the PI$^{\bullet-}$ or NI$^{\bullet-}$ absorption bands and the decay of the bands over a few tens of nanoseconds.

Factor two is evident by a long-lived absorption in the transient absorption kinetics of all four dyads, which we assign to a triplet state that is formed upon back electron transfer. This long-lived feature was also previously observed with the dyad 6P-NI.[9] Since the formation time of the ion pairs occurs on a sub-picosecond time scale, and the excited-state lifetime of the donors is 8.5 ns, the yields of triplet states formed through SO-ISC are negligible and must be derived from back electron transfer. Further evidence supporting this conclusion is that the phosphorescence quantum yield of the 6P-NI dyad is about 100 times greater than that of the donor 6P alone.[9] The emission spectrum for 6P-NI appears nearly identical to the triplet of NI, showing that the final triplet lies on NI, i.e., [6P-^{3*}NI]. We again ascertained similar characteristics for all of the dyads, including the phosphorescence decay times shown in Table 3. Another experiment that precludes mechanisms for the intense phosphorescence of the dyads, other than back electron transfer, can be realized by using a closely related dyad that cannot undergo electron transfer, e.g., 5P-PhI. Figure 2 illustrates the CW emission spectra for 5P-PhI and 5P-PI at 77 K in 2-MTHF. It illustrates that 5P-PhI does not phosphoresce, but that the dyad 5P-PI phosphoresces significantly due to the back electron transfer reaction to form a triplet. Here, the triplet state of the 5P donor is ultimately populated, since the ^{3*}PI state is higher in energy. The 5P control molecule alone does not show phosphorescence. This experiment, in conjunction with the 100% quantum yield of the radical pairs in the dyads, eliminates the possibility of an increase in the phosphorescence quantum

(17) Gonen, O.; Levanon, H. *J. Chem. Phys.* **1986**, *84*, 4132−41.
(18) Regev, A.; Galili, T.; Levanon, H. *J. Phys. Chem.* **1996**, *100*, 18502−18510.
(19) Greenfield, S. R.; Wasielewski, M. R. *Opt. Lett.* **1995**, *20*, 1394.
(20) Greenfield, S. R.; Svec, W. A.; Gosztola, D.; Wasielewski, M. R. *J. Am. Chem. Soc.* **1996**, *118*, 6767−6777.
(21) Ramaswamy, M.; Ulman, M.; Paye, J.; Fujimoto, J. G. *Opt. Lett.* **1993**, *18*, 1822−4.
(22) Pshenichnikov, M. S.; Boeij, W. P. d.; Wiersma, D. A. *Opt. Lett.* **1994**, *19*, 572−74.

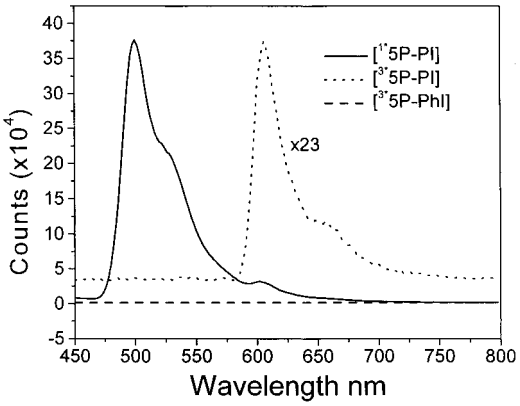

Figure 2. The CW phosphorescence spectra for 5P-PhI and 5P-PI at 77 K in MTHF are shown, along with the fluorescence spectrum from 5P-PI. The 5P-PI dyad that is capable of undergoing electron transfer shows phosphorescence, while 5P-PhI does not show phosphorescence. This is further evidence that the triplet excited state is populated only through back electron transfer.

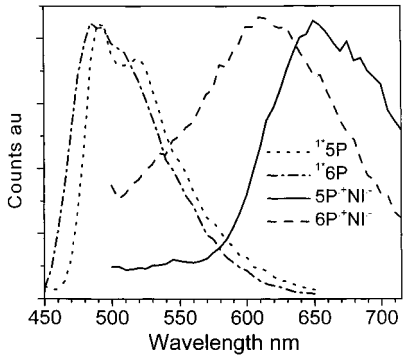

Figure 3. The TCSPC spectra for 5P (0 ns delay), 6P (0 ns delay), 6P-NI (30 ns delay), and 5P-NI (30 ns delay) in MTHF at 77 K clearly illustrate the different energies of the radical pairs, with the [$6P^{\bullet+}$-$NI^{\bullet-}$] emission band at 610 nm and the [$5P^{\bullet+}$-$NI^{\bullet-}$] emission band at 650 nm.

yield in the dyads due to changes in SO-ISC relative to the donors and acceptors alone.

Factor three is characterized by charge transfer emission bands that enable the determination of the absolute values of the radical pair energies in different phases. These bands are especially evident for the two lowest energy radical pairs, [$6P^{\bullet+}$-$NI^{\bullet-}$] and [$5P^{\bullet+}$-$NI^{\bullet-}$], as shown in Figure 3 in 2-MTHF at 77 K. These bands clearly show that the energy of the [$5P^{\bullet+}$-$NI^{\bullet-}$] radical pair emission centered at 660 nm (1.88 eV) is lower than the corresponding [$6P^{\bullet+}$-$NI^{\bullet-}$] emission centered at 610 nm (2.03 eV). Another important aspect of the emission bands is their broad energy range with fwhm values on the order of 0.3 eV and total widths of about 0.6 eV. We will show that this breadth in energy levels has important ramifications for the mechanism of charge transfer and charge recombination reactions. Charge-transfer emission from [$5P^{\bullet+}$-$PI^{\bullet-}$] and [$6P^{\bullet+}$-$PI^{\bullet-}$] is also discernible at shorter wavelengths (570 and 540 nm, respectively), but the emission intensities are much weaker.

The photoinduced processes within the dyads described above in frozen glasses are illustrated in a general energy level scheme shown in Figure 4. In the glass phase, the optical data indicate that all four radical pairs lie above the triplet energy levels of their components, i.e., donors and acceptors, and that charge recombination occurs to the lowest triplet state within the molecule, i.e., ^{3}*NI for NI containing molecules, and ^{3}*5P or ^{3}*6P for molecules containing PI. We find through CW

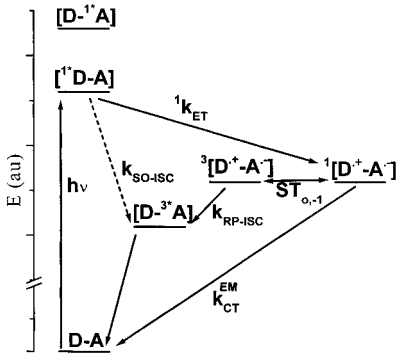

Figure 4. An energy level diagram for the donor−acceptor (D-A) dyads at low temperatures illustrates the different photoinduced processes that occur in these molecules. The triplet state that is reached through RP-ISC can be localized on either the donor or the acceptor, i.e., [D-^{3*}A] or [^{3*}D-A]. The triplet radical pair is formed through both S-T_0 or S-T_{-1} mixing, designated in the figure as ST_{0-1}. EM refers to emission.

phosphorescence measurements that the energy level of ^{3}*PI lies at 2.45 eV, well above the triplet states of 5P or 6P. Since these molecules have a much shorter charge separation distance than previously studied systems exhibiting back electron transfer to a triplet state, we turn to TREPR studies to elucidate this process.[6−8]

TREPR in Liquid Crystals at Low Temperatures. The kinetics of the radical pair recombination reaction deduced from the optical spectroscopic measurements show that the time for charge recombination in the dyads is too short to observe the radical pair in TREPR experiments at low temperature. However, we can observe the ESP patterns of the triplet states created by back electron transfer to learn more about the mechanism for RP-ISC. We will refer frequently to the energy level diagrams shown in Figure 5a−c for the temperatures 170, 240, and 300 K. These temperatures correspond to crystalline, soft glass, and nematic phases of E-7, respectively. The energy levels are drawn to take into account all of the optical and TREPR data.

The TREPR data for the dyads and the individual moieties reveal a novel mechanism for mixing of the singlet and triplet sublevels to produce a polarized triplet spectrum.[2,23] We will show that this is a function of the short radical pair distance and the high J values associated with these systems. The acquired data are a result of using LCs, because the information content of employing isotropic glasses is not as high as with LC oriented samples where spin dynamics can also be monitored.[24] Figure 6 shows the triplet spectra of 5P and NI, along with their simulations. 6P exhibits an extremely weak triplet signal so that the polarization pattern is difficult to discern. PI does not absorb any light at 420 nm, precluding the observation of a triplet signal. The triplet spectrum of 5P exhibits a clear ESP pattern of *e a* for the parallel orientation (**L**||**B**), and an *e e a a* pattern for the perpendicular one (**L**⊥**B**), where *e* and *a* stand for enhanced emission and absorption, respectively. For 5P it was found that $|D| = 495 \times 10^{-4}$ cm^{-1} and $|E| = 28 \times 10^{-4}$ cm^{-1}. In the **L**||**B** configuration, the out-of-plane canonical axis does not contribute to the spectral intensity due to the negligible probability to find the molecular plane perpendicular to the director. The two in-plane axes should contribute to the spectrum with line intensity ratio depending on the angle ϕ_0.[17,18] Since ϕ_0 is 45°, both the *x*- and *y*-axes should contribute equally to the EPR spectrum for **L**||**B**. The simulation of the EPR

(23) Levanon, H.; Norris, J. R. *Chem. Rev.* **1978**, *78*, 185.
(24) Levanon, H.; Hasharoni, K. *Prog. React. Kinet.* **1995**, *20*, 309−46.

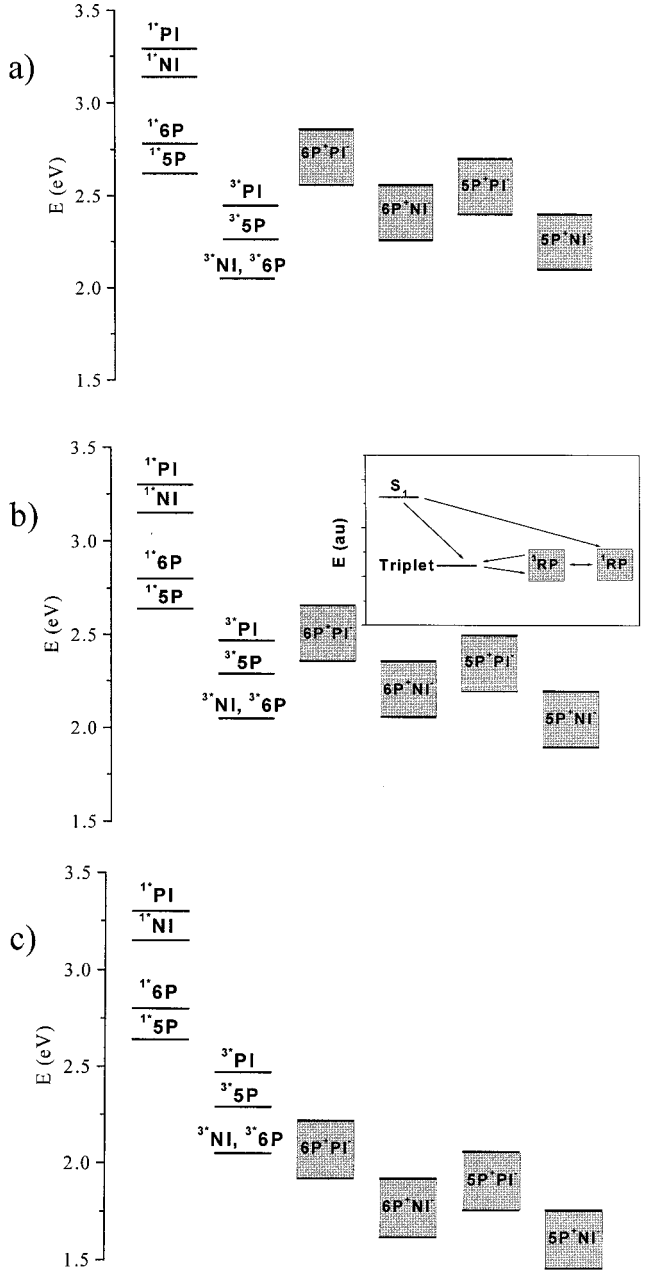

Figure 5. The energy level diagrams for the radical pair energies are shown for the (a) glass phase at 170 K, (b) soft glass phase at 240 K, and (c) liquid crystal phase at 300 K.

spectrum shows that the triplet population rate along the *y*-axis, A_y, is far greater than A_x (Table 2). Thus, only one set of lines is observed in the **L**||**B** spectrum. The *x*- and *z*- axes populations are evident in the **L**⊥**B** spectrum. The combined *e e e a a a* pattern is consistent with the SO-ISC mechanism for triplet formation.[2,23] The triplet state of NI exhibits the identical ESP pattern and the strong triplet signal is consistent with the higher phosphorescence quantum yield for ^{3}*NI relative to the donor species.

Realizing that the triplet signals of the monomeric species are due to SO-ISC, we can now more fully appreciate the very unusual polarization patterns present in the dyads. 5P-PI and 6P-PI exhibit polarized triplet spectra with an *a e* pattern for the **L**||**B** orientation and an *a a e e* pattern for the **L**⊥**B** one. Thus, an overall polarization pattern is *a a a e e e*, as illustrated in Figure 7, along with the simulations. These polarization patterns are opposite to that of 5P, with the *D* values for the

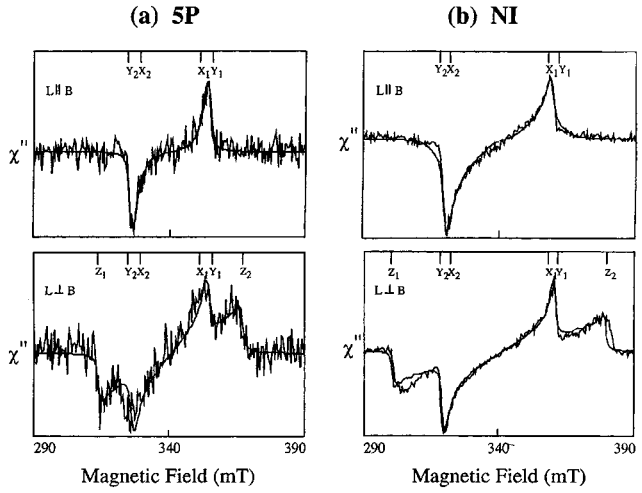

Figure 6. The TREPR spectra (~1 ms after photoexcitation) at 170 K in E-7 for (a) ^{3}*5P and (b) ^{3}*NI are shown.

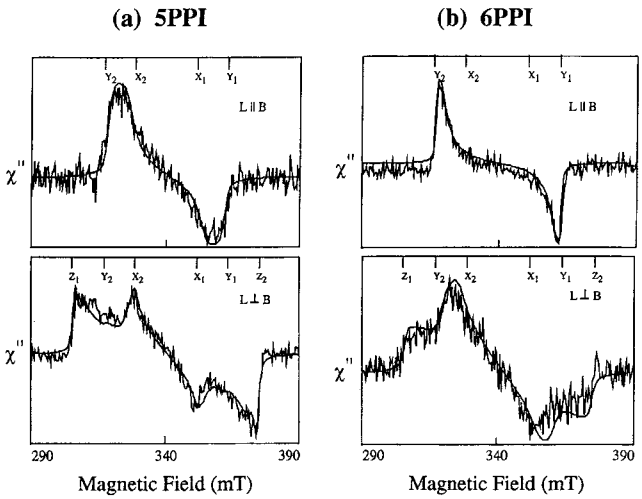

Figure 7. The TREPR spectra (~1 ms after photoexcitation) at 170 K in E-7 for (a) ^{3}*[5P-PI] and (b) ^{3}*[6P-PI] are shown.

dyads ($|D| = 645 \times 10^{-4}$ cm^{-1}) larger than those for 5P ($|D| = 495 \times 10^{-4}$ cm^{-1}). It should be reiterated that the triplet signal from 6P is very weak, and assignment of the polarization pattern is difficult, although it seems to be similar to that of 5P. We reiterate that the triplet energy of PI is higher than that of 5P or 6P, so that the triplets of the dyad molecules are localized on the donor moieties, i.e., [^{3}*5P-PI] or [^{3}*6P-PI]. However, the significant change in *D* values indicates that the triplet energy of the dyads is confined to a smaller portion of the molecules. We believe this is due to the fact that the control molecules (5P and 6P) do not function as "perfect" controls for the dyads. 5P and 6P possess tolyl groups that replace the electron acceptors NI and PI. The dihedral angle between the plane of the tolyl group and that of the naphthaleneimide ring in 5P and 6P is smaller relative to the corresponding dihedral angle between the donor and acceptor moieties in the dyads because of steric hindrance between the carbonyl groups. Thus, an additional degree of electron delocalization to the tolyl groups occurs in ^{3}*5P and ^{3}*6P that is not present in the dyad triplet states.

When the acceptor NI replaces PI in the dyads, the parallel and perpendicular spectra exhibit *a e* and *e e a a* patterns, respectively, with an overall *e e a e a a* pattern (Figure 8). It is important to note that unlike the triplets of 5P-PI and 6P-PI, the triplet spectra of 5P-NI and 6P-NI are similar to that of NI,

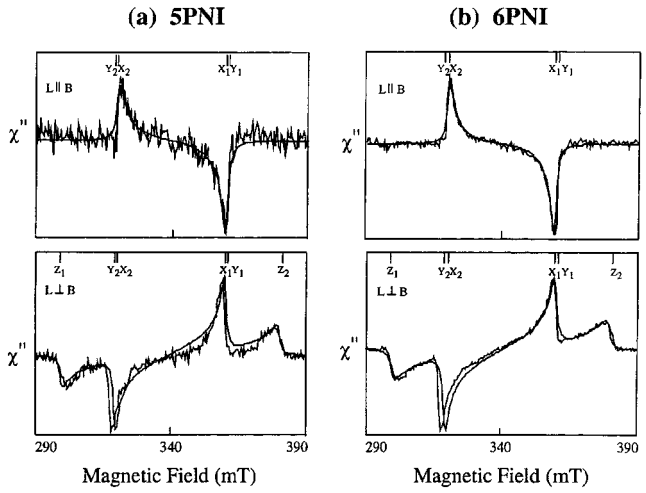

Figure 8. The TREPR spectra (~1 ms after photoexcitation) at 170 K in E-7 for (a) ^{3}*[5P-NI] and (b) ^{3}*[6P-NI] are shown.

particularly in the perpendicular orientation. The major difference between the triplet spectra of 5P-NI and 6P-NI compared to NI is the different polarization pattern of the parallel spectrum (**L**||**B**) and, to some extent, the ZFS parameters. The ZFS parameters and the optical data indicate the triplet in these cases lies on NI, i.e., [D-^{3}*NI], where D is 5P or 6P (Table 2).

As we discussed above, optical studies indicate unambiguously that in all dyads under study, singlet-initiated electron transfer occurs rapidly and with high yield, precluding the possibility of SO-ISC. In such a case the observed TREPR triplet spectra of the dyad molecules cannot be regarded as originating from SO-ISC. The only other possibility to produce the observed triplet spectra is RP-ISC, as a result of the charge recombination process, i.e., back electron transfer. Nevertheless, the ESP patterns of ^{3}*[D-A] in any of the dyads are not consistent with RP-ISC resulting from S-T_0 mixing, i.e., *a e e a a e* (or *e a a e e a*).[23] The latter is observed only in the photosynthetic reaction center and in some large biomimetic model systems.[6−8] RP-ISC in the case of S-T_0 mixing results in an *a e e a a e* polarization pattern, due to overpopulation of the T_0 state at all canonical orientations. In a similar manner, RP-ISC with S-T_{-1} mixing results in an *e a a e e a* polarization pattern (opposite to that of S-T_0 mixing) due to overpopulation of the T_{-1} state. The ESP patterns, exhibited by ^{3}*[D-A], i.e., *a a a e e e* in the case of 5P-PI and 6P-PI, and *e e a e a a* in the case of 5P-NI and 6P-NI, are not consistent with either of these cases. The possible explanation for this discrepancy may be found in the assumption that the close proximity of the electron spins within [$D^{\bullet+}$-$A^{\bullet-}$] creates the situation in which J is large enough to permit both S-T_{-1} and S-T_0 RP-ISC to occur. This mixing is accompanied by anisotropic spin−lattice relaxation at the three canonical orientations of the triplet state.

To account for these unique observations, fast anisotropic spin lattice relaxation must occur on EPR time scales. We start first by analyzing the spectrum shown in Figure 8 by inspection of the energy level diagram of Figure 9. Two cases must be considered: the S-T_0 and S-T_{-1} mixing. In the first case (Figure 9a), by assuming that the population decay rates of the z and y canonical orientations are faster than the EPR detection time, the x canonical orientation (identified with T_0) is overpopulated, and in the RP-ISC mechanism the y and z canonical orientations (each identified with T_0) are not populated. This results in a spectrum where only the x-transitions are detected, namely, o_z,e_x,o_y,o_y,a_x,o_z where o_i ($i = x, y, z$) indicates zero line intensity in the particular canonical orientation. As stated above, we must

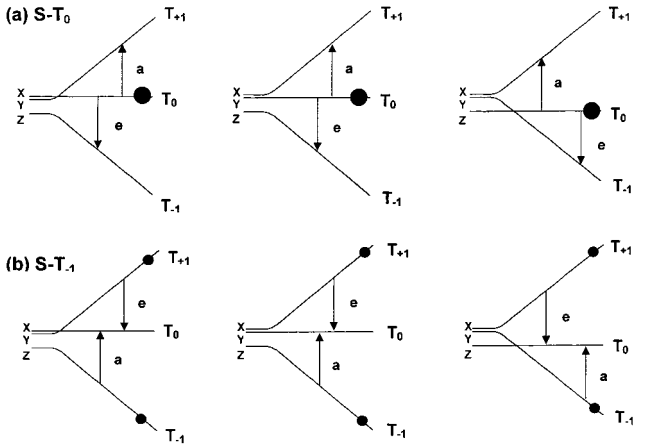

Figure 9. The energy level diagram illustrating two cases of mixing: (a) the S-T_0 and (b) S-T_{-1} mixing.

also consider the S-T_{-1} mixing as shown in Figure 9b. By employing the same assumption of fast depletion of the z and y states, one will end up with the spectrum e_z,o_x,a_y,e_y,o_x,a_z. Thus, the overall spectrum will be e_z,e_x,a_y,e_y,a_x,a_z, which agrees with the experimental observations (Figure 8). It should be emphasized that the above analysis holds for [D-^{3*}NI], where D is 5P or 6P.

This anisotropy is readily apparent by comparing Figures 6b and 8 for [D-^{3*}NI] by noting that the intensity of the low-field line in the **L**||**B** spectrum of ^{3*}NI is greater than that of the high-field line, while the opposite is true for [D-^{3*}NI]. In Figure 7 the triplet spectra of 5P-PI and 6P-PI are shown. In this case it is evident that the general line shape exhibits an a/e pattern, which is typical for out-of-plane selective population, i.e., active z-axis. Similar to the treatment of the D-NI dyads, we assume that the fast depletion is from y and x levels in the D-PI dyads. This leaves us with a spectrum for S-T_0 mixing of a_x,o_x,o_y,o_y,o_x,e_z and o_z,a_x,a_y,e_y,e_x,o_z for the S-T_{-1} mixing, with an overall spectrum a_z,a_x,a_y,e_y,e_x,e_z, which again is in full agreement with the experimental observations.

A quantitative line shape analysis was carried out on each dyad. Each system was assigned by a frame-of-reference located on the triplet chromophore. Inspection of Table 2 indicates that the ZFS in ^{3*}NI and [D-^{3*}NI] are very close. However, the population rates of the dyads are different from those of the monomer, which is reflected by the phase pattern of the different signals. Also of interest is the breadth of the triplet line shape of 5P-PI relative to 6P-PI at 170 K. This may indicate that the rotational freedom for the pyrrolidinyl ring of 5P-PI is greater than that for the piperidinyl ring of 6P-PI at 170 K.

It should be noted that the large values of ϕ_o for the dyads of 60° to 70° used for the simulations indicate that these molecules do not align parallel to the LC director **L**. The same was shown for similar, albeit larger, molecules and was interpreted in terms of p-stacking.[7] On the other hand, the out-of-plane z-axes do not manifest themselves in the parallel spectra. Thus, an overall cylindrical distribution of stacked molecules around **L** may be surmised, despite the ~90° dihedral angle between the two moieties.

TREPR in the Soft Glass and Fluid Phases. The soft glass region of E-7 demonstrates large changes in the ability to solvate an ion pair as a function of temperature. Thus, this environment permits an unusual opportunity to carefully monitor solvation changes as the solid takes on liquid character over a temperature range of 53 deg. We start the analysis of the TREPR spectra in this region with the 5P-NI dyad, which possesses the ion pair,

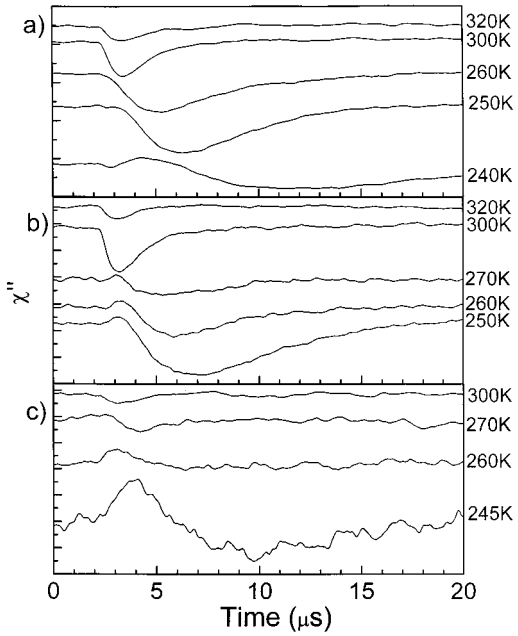

Figure 10. (a) The kinetics of ^{3}[5P$^{\bullet+}$-NI$^{\bullet-}$] (in the low field part of the spectrum) at differing temperatures are illustrated. (b) The kinetics of ^{3}[6P$^{\bullet+}$-NI$^{\bullet-}$] (in the low field part of the spectrum) at differing temperatures are illustrated. (c) The kinetics of ^{3}[5P.$^+$-PI.$^-$] (in the low field part of the spectrum) at differing temperatures are illustrated.

[5P$^{\bullet+}$-NI$^{\bullet-}$], with the lowest energy. At 223 K, which is the low temperature region of the soft glass phase, only the triplet of 5P-NI is observed, which decreases in intensity as the temperature increases. Over the temperature region that the triplet is observed, i.e., <250 K, no change of the polarization pattern occurs, indicating that the triplet formation is still due to back electron transfer and thus at least some of the radical pair energy levels lie above the triplet (Figure 5b).

At 240 K the narrow signal superimposed on the weak triplet spectrum starts to build up. This signal is attributed, similarly to previously studied dyad systems with short donor−acceptor distances, to the triplet radical pair (TRP), ^{3}[5P$^{\bullet+}$-NI$^{\bullet-}$].[9] The emergence of this signal means that at least part of the radical pair energy level band drops below the [5P-^{3*}NI] energy, so that back electron transfer to the triplet is not thermally accessible and back electron transfer to the ground state begins to occur. The nearly 2 eV free energy change places this back electron-transfer reaction in the Marcus inverted regime and the reaction slows down dramatically.[25,26] The ZFS parameter D of ^{3}[5P$^{\bullet+}$-NI$^{\bullet-}$] is ∼10 mT, and applying the dipole approximation permits the estimation of the donor−acceptor distance r = 6.55 Å, which is in good agreement with the molecular geometry.[24]

The radical pair kinetic curves for ^{3}[5P$^{\bullet+}$-NI$^{\bullet-}$] illustrated in Figure 10a exhibit strong temperature dependence. At 240 K, the initial emission (e_1) is followed by an absorption and ultimately by a second emission (e_2). The phase inversion corresponds to the existence of different routes for producing the radical pair states, i.e., singlet and triplet initiated routes.[15,24] Therefore, the two emissive radical pair signals must be due to two different triplet-initiated radical pair routes. Two possible routes for the triplet-initiated radical pair formation can be understood by observing the inset Figure 5b. One manner by which a triplet-initiated radical pair can be created is a result of the slower electron-transfer rate in the soft glass due to the "nematic potential" that is introduced.[24] The nematic potential actually slows the forward electron-transfer rate enough to permit some ordinary SO-ISC, to produce [5P-^{3*}NI]. Subsequent electron transfer from [5P-^{3*}NI] to produce [5P$^{\bullet+}$-NI$^{\bullet-}$] occurs as well. The decrease in the electron-transfer rate has already been shown through transient absorption spectroscopy to be on the order of a factor of 400, permitting time for SO-ISC.[27] The second mechanism for triplet formation is to populate the higher energy levels of the ^{1,3}[5P$^{\bullet+}$-NI$^{\bullet-}$] band from the singlet state of ^{1*}[5P-−NI], which can then back react to form [5P-^{3*}NI]. Because of the broad nature of the radical pair bands, the [5P-^{3*}NI] state can initiate electron transfer to the lower lying radical pair states of the band to create triplet-initiated radical pairs.

The second mechanism requires the formation of singlet initiated radical pairs that produce the absorption so that back electron transfer to the triplet state can occur, and is thus the likely source of the e_2 emission. This leaves SO-ISC as the source of the e_1 emission. Note that the triplet itself is not observed for either mechanism due to population depletion from triplet-initiated electron transfer to form the radical pairs. Upon a temperature increase to 250 K, the radical pair kinetics is dominated by one emission. SO-ISC is now the dominant mechanism for the radical pair emission signals because the radical pair band begins to drop below the triplet state, eliminating the possibility of back electron transfer to the triplet state. The mechanisms responsible for the absorption and e_1 emission at 240 K are still weakly active, but begin to cancel each other. This leads to the long delay between the photoexcitation time at ∼2 ms and the appearance of the e_2 emission at ∼4 ms. The higher energy of [6P$^{\bullet+}$-NI$^{\bullet-}$] relative to [5P$^{\bullet+}$-NI$^{\bullet-}$] is evident in the radical pair kinetics shown in Figure 10b. Here, the singlet-initiated radical pair absorption signal is evident up to 270 K as compared to 250 K for [5P$^{\bullet+}$-NI$^{\bullet-}$]. Furthermore, no [6P$^{\bullet+}$-NI$^{\bullet-}$] signal is evident until 250 K, as compared to 240 K for [5P$^{\bullet+}$-NI$^{\bullet-}$].

We now discuss the radical pair kinetics of 5P-PI and 6P-PI. The back electron-transfer reaction produces [^{3*}D-PI] because ^{3*}PI lies above ^{3*}D. The kinetics of 5P-PI differ from those of 5P-NI and 6P-NI (Figure 5b) because the ^{3*}5P energy level is 0.24 eV higher than the ^{3*}NI triplet level. Thus, the back electron-transfer reaction returns to a higher energy level than for the dyads that contain NI. This results in the onset of signal at lower temperature than for [6P$^{\bullet+}$-NI$^{\bullet-}$], even though the energy level of [6P$^{\bullet+}$-NI$^{\bullet-}$] is lower than that of [5P$^{\bullet+}$-PI$^{\bullet-}$]. The radical pair kinetics for 5P-PI are illustrated in Figure 10c. At 245 K, an absorption signal is observed at early times, and indicates singlet-initiated electron transfer. This is followed by an emission signal that is due to triplet-initiated radical pairs. Thus, in the soft glass phase, the radical pair energy level overlaps with the ^{3*}5P energy level. At the higher nematic phase temperatures, only an emission signal is observed, indicating that only triplet-initiated electron transfer is operative and that the radical pair energy level band has dropped entirely below the ^{3*}5P level.

For the case of 6P-PI, no radical pair signal could be observed at any temperature. However, the broad triplet spectrum of 6P-PI was observed up to 255 K, becoming weaker upon increasing the temperature. The optical data show that any triplet present in the frozen glass is a result of back electron transfer because the PI$^{\bullet-}$ moiety is formed in less than 1 ps in the glass phase with a recombination time of 64 ns. At 260 K, the high-temperature region of the soft glass phase, the triplet signal

(25) Marcus, R. A. *J. Chem. Phys.* **1956**, *24*, 966.
(26) Marcus, R. *J. Chem. Phys.* **1965**, *43*, 679−701.
(27) Wiederrecht, G. P.; Svec, W. A.; Wasielewski, M. R. *J. Am. Chem. Soc.* **1997**, *119*, 6199−6200.

Table 4. The Center Energy Level of the Radical Pair States in the Frozen and Soft Glass Phases

temp, K	[5P$^{\bullet+}$-PI$^{\bullet-}$], eV	[6P$^{\bullet+}$-PI$^{\bullet-}$], eV	[5P$^{\bullet+}$-NI$^{\bullet-}$], eV	[6P$^{\bullet+}$-NI$^{\bullet-}$], eV
170	2.55	2.71	2.25	2.41
240	2.35	2.51	2.05	2.21
245	2. 29	2.45	2.19	2.15
250	2.15	2.31	1.85	2.01
300	1.91	2.07	1.61	1.77

disappears completely due to fast quenching by electron transfer as described above.

Table 4 cites the center energy level of the four radical pairs in the glass, soft glass, and liquid crystal phases. The values use the arguments cited above for the appearance of the signal, indicating energy overlap with optically determined triplet excited-state energy levels. The disappearance of the triplet signal due to fast depopulation and the triplet-initiated polarized emission signals also assist with the energy level assignments because it implies that the radical pair level has dropped below the triplet excited state. Finally, the redox values cited in Table 1 set the relative difference by which each radical pair level must differ. Therefore, if the lowest level radical pair [5P$^{\bullet+}$-NI$^{\bullet-}$] is established to drop just below the energy level of ^{3}*NI (2.05 eV) at 240 K, then the [5P$^{\bullet+}$-PI$^{\bullet-}$] energy level must lie 0.3 eV higher, based upon the redox potential differences of the donor and acceptor. The sign of the polarized TREPR signals matches the energy level assignment. Given the small energy gaps of the radical pairs and triplet states, these energy levels are accurate to $\pm$0.05 eV. The destabilization of the radical pair in the solid state relative to the liquid crystalline phase is 0.65 eV, in good agreement with previously measured values.[1]

Conclusions

We have presented optical and TREPR data on a series of short distance, covalently bound donor−acceptor dyads. These dyads possess the shortest donor−acceptor distances for which radical ion pair phenomena have been probed by EPR. We have shown that they (1) undergo ultrafast charge separation ($\sim$1 ps) from the photoexcited singlet excited state of the donor at low temperature; (2) possess charge transfer bands in the visible region, a rarity among dyads in which the donor and acceptor are not significantly electronically coupled in the ground state; (3) possess the rare characteristic that they back electron transfer to a triplet state at low temperature; (4) possess a novel mechanism for RP-ISC as judged by the unique polarization patterns of the resulting triplet states; and (5) that aligned liquid crystals are advantageous for these studies. The final point is a consequence of the ability of LCs to undergo a gradual transition from a glassy state to a liquid crystal phase. This permits precise measurements of radical pair energy levels and solvation energies, and slows the radical pair reaction rates sufficiently so that observation of a TREPR signal from the radical pair is possible.

Acknowledgment. We are grateful to Mr. A. Blank for helpful discussions. This work was supported by the Division of Chemical Sciences, Office of Basic Energy Sciences, U.S. DOE under grant No. DE-FG02-99ER14999 (M.R.W.) and contract W-31-109-ENG-38 (W.A.S.). This work was also supported by the Office of Advanced Scientific Computing Research, U.S. DOE under contract W-31-109-ENG-38 (G.P.W.). The research described herein was also supported by U.S.-Israel BSF (H.L., M.R.W.) and by the Volkswagen Stiftung, and by the DFG (SFB program 337) (H.L.). The Farkas Center is supported by the Bundenministerium für Forschung and Technologie and the Minerva Geselschaft für die Forschung GmbH.

Supporting Information Available: Syntheses of 5P-NI and 5P-PhI (PDF). This material is available free of charge via the Internet at http://pubs.acs.org.

JA000662O